QUALIFICATION OF SILANE COATINGS FOR THE STRENGTH ENHANCEMENT OF CONCRETE PARTS

C. Hahm[1], R. Theska[1], D. Raab[1], A. Fehringer[2], M. Mitterhuber[3], A. Kästner[3]

[1]Technische Universität Ilmenau, Germany, Department of Mechanical Engineering
[2]Egbert Reitz Natursteintechnik e.K., Germany
[3]ETC-Products Gmbh, Germany

ABSTRACT

In former own publications [2]..[6] it was shown, that high precision concrete parts are a reliable alternative to natural stone for machine base frames. Beside long-term stability, also a predictable and highly reproducible thermal behavior is required. One opportunity is the application of materials with identical thermal expansion coefficients and appropriate mechanical properties. Concrete is a promising material for the whole machine structure under these circumstances.

In contrast to base frames, moving parts need to have a lightweight design thus requiring a high level of specific stiffness. Concrete with a specific stiffness close to steel is an interesting material for the design of movable components coming up with dynamic properties comparable to welded steel structures. Additionally a high material strength is needed in lightweight design. To guarantee reliability at the same level as steel or aluminum light-weight parts, the endurance strength of concrete parts has to be improved significantly.

Index Terms - Precision concrete, endurance strength enhancement,
lightweight construction, organo-functional surface coating

1. INTRODUCTION

For the implementation of a predictable and highly reproducible thermal behavior the use of low expansion materials is not appropriate for a whole machine structure since they are coming up with several drawbacks in the mechanical behavior in combination with high costs. Thermal compensation by special design raises complexity and costs as well. The application of special concrete compositions allowing both massive and filigree structures with identical thermal expansion coefficients can solve this problem at significantly reduced costs.

The main challenge for the development of concrete light-weight parts is the improvement of the endurance strength, because concrete shows high compressional strength but is very sensitive to tensile stress. The tensile load at complex geometry cannot be fully eliminated. Therefore, notch effects and stress concentrations need to be avoided. Reinforcement by implementation of steel or carbon fibers is not applicable since it comes with thermal inhomogeneity.

As an alternative, reinforcement can also be derived by functional coating. The application of a tailor made sol-gel coating with enhanced tensile strength like organo-functional silane implements compressive preload to the parts surface. Furthermore, the tensile strength in the sol-gel-infiltrated zone is improved and surface micro damages are filled out. These three fundamental effect mechanisms and the coherences to the endurance strength are shown in the chart at figure 1.
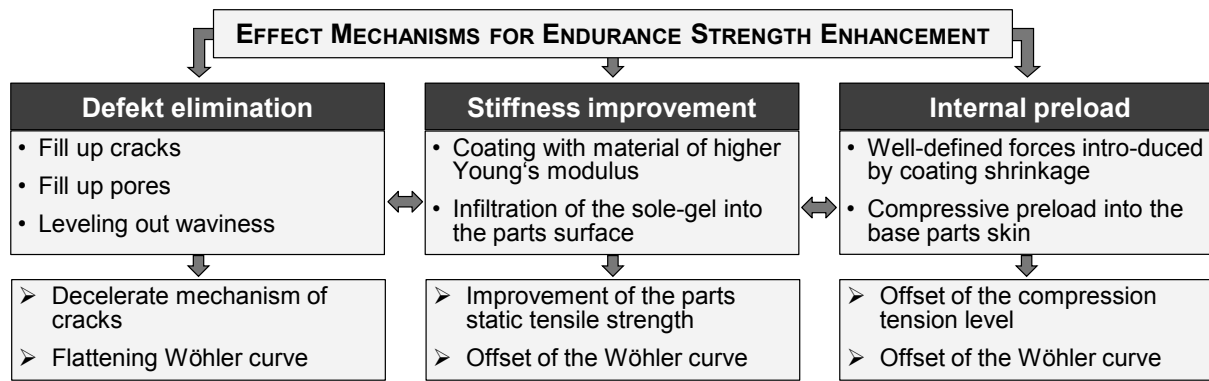
EFFECT MECHANISMS FOR ENDURANCE STRENGTH ENHANCEMENT		
Defekt elimination	**Stiffness improvement**	**Internal preload**
• Fill up cracks • Fill up pores • Leveling out waviness	• Coating with material of higher Young's modulus • Infiltration of the sole-gel into the parts surface	• Well-defined forces intro-duced by coating shrinkage • Compressive preload into the base parts skin
➢ Decelerate mechanism of cracks ➢ Flattening Wöhler curve	➢ Improvement of the parts static tensile strength ➢ Offset of the Wöhler curve	➢ Offset of the compression tension level ➢ Offset of the Wöhler curve

Figure 1. Effects for strength enhancement of sol-gel coated parts

To verify the impact of the defect elimination, supporting factors as used in the German FKM Guidelines [7] can be applied beneficially. Since the measurement of internal stresses in the surface surrounding area is not possible for concrete without taking effect to the internal stresses itself, the mathematical description of the stiffness improvement is a promising approach to verify the influence of the coating.

2. METHODOLOGY

The prediction of the endurance strength enhancement for functional coated concrete parts is based on a combination of calculated and experimentally derived data. The measurement data are influenced by all effects and cross interactions and cannot be fully separated.

For the endurance strength prediction of sol-gel coated concrete parts in lightweight design, the effective use of an appropriate FE-model method is helpful. First, the whole geometry has to be modeled in form of volume elements. The main result of the coating is an increased stiffness. To imply this effect, the coating properties are simulated by surface shell elements with coincident nodes to the volume elements at the rim of the base part. After the application of surface shell elements a reinforcement of the part is achieved. The derived displacements for the non-coated and the coated state are in correspondence to the relative stress level. With the relative stress level the prediction of the endurance strength enhancement for complex geometry is possible. To implement a simple shell element type for the description of the coated parts properties a substitute thickness T_{subst} and a representative Young's modulus E_{subst} needs to be introduced. The determination of these parameters is done based on a simplified prismatic beam model. The parameters are gained within the following three steps.

1. Mathematical description of the physical properties
2. Experimental determination of measurable properties
3. Calculation of the remaining physical properties

The procedure for the implementation of physical properties and coating parameters for the prediction of the endurance strength enhancement will be shown in the next chapter. The composition of the sol-gel-system and the regard of the influences of the chemical and physical properties of the sol in the model are currently under process and not part of this contribution.

3. MATHEMATICAL DESCRIPTION

The mathematical description of the stiffness of a coated prismatic geometry is done by an analytic model using a variable Young's modulus over the cross section. The Young's modulus at the rim of the base part and at the outside of the coating is not directly measurable.
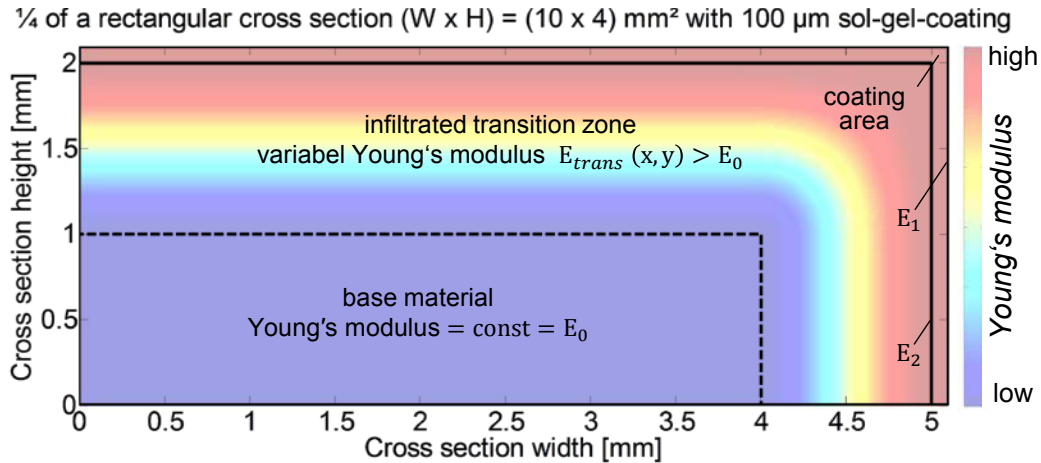
¼ of a rectangular cross section (W x H) = (10 x 4) mm² with 100 µm sol-gel-coating

Figure 2. *Young's modulus distribution in a rectangular cross section*

An exemplary distribution of the Young's modulus in a rectangular cross section is shown in figure 2. Based on the estimation that the stiffness can't change abruptly over the position the stiffness change is expressed in form of a harmonic approximation [1]. The Young's modulus in the area limited by the dashed line is the base part Young's modulus E_0. The Young's modulus at the outside of the coating is called E_1. In the infiltrated transition zone the Young's modulus changes from E_0 to the maximum E_2 at the rim of the base part represented by the solid line.

The example beam is 10 mm in width W, 4 mm in height H and 35 mm long. The measures of the coating influenced areas are the infiltrated depth RHT of 1 mm and the 100 µm wall thickness T of the coating. The determination of E_1 and E_2 is explained in the following steps.

4. EXPERIMENTAL INVESTIGATIONS

The mechanical tests are executed with standardized shouldered specimen geometry of *DIN 50125 Form - E 4 x 10 x 35* (figure 3). A section with a length L of 35 mm in the center of the 45 mm long parallel specimen segment is analyzed for the displacement measurements.
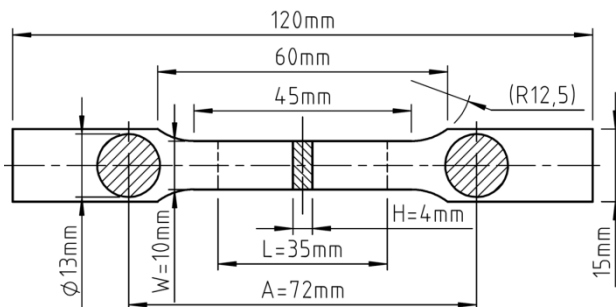

Figure 3. *dimensions of the shouldered specimen*

The dimensions W and H of the specimen are determined by the mean value of 4 measures along the beams. The tensile load test and the 3-point flexure test yield two different values of the stiffness.

If the Young's modulus is constant at the cross-section of a specimen, these two measurements are leading to equal Young's modulus values. So the determination of the uncoated Young's modulus E_0 is only been done with the tensile test. For the determination of E_1 and E_2 of the coated specimen both measurement setups are necessary. The cubic term of the height coordinate in the moment of inertia for the bending load case generates an independent equation for the stiffness calculation. Since all geometrical dimensions of the cross-sections influenced by the coating are given, the distribution of a varying Young's modulus along a cross-section can be done with the determination of the tensile stiffness $C_{tensile}$ and the flexural stiffness $C_{flexure}$.

The infiltrated depth is measured by UV and X-ray fluorescence microscopy of broken specimen cross sections. The coating thickness is determined by mechanical profilometry.

4.1 Experimental setups

4.1.1 Determination of the infiltrated depth and the coating thickness

The determination of the infiltrated depth was done by UV and X-ray fluorescence. For this detection method it was necessary to apply a fluorescence colorant.

Primarily the test cubes were moistened with the following solutions:

- $SnCl_2$ in isopropanol,
- fluorescent CanDot in water
- fluorescent CanDot in hexane

An ultraviolet lamp with a fluorescence stimulating wavelength range from 254 to 366 nm was used for the detection of the CanDot-solutions. $SnCl_2$ was detected with the Fischer-device XDV-SDD.

The determination of the coating thickness was done by mechanical profilometry with an Alpha-Step IQ (company KLA-Tencor). This device is a computerized, high-sensitivity surface profiler with 2.5 µm stylus diameter. The measuring distance was about 2 mm and the detection speed took about 50 µm/s.

4.1.2 Tensile test arrangement

The specimen *Form E 4 x 10 x 35* made of concrete can't serve the demands of the *DIN 50125* for steel specimen and are very sensitive to parasitic lateral forces and inertias. To avoid influences of the clamping and machine misalignments a special clamping is needed. With spherical chucks shown in figure 4 the alignment of the clamp to the specimen axis is possible. The chucks are specially fitted, that the center of the spheres are nearly coincident to the specimen's axis. Therefor the influence of parasitic lateral forces and inertias is minimized.
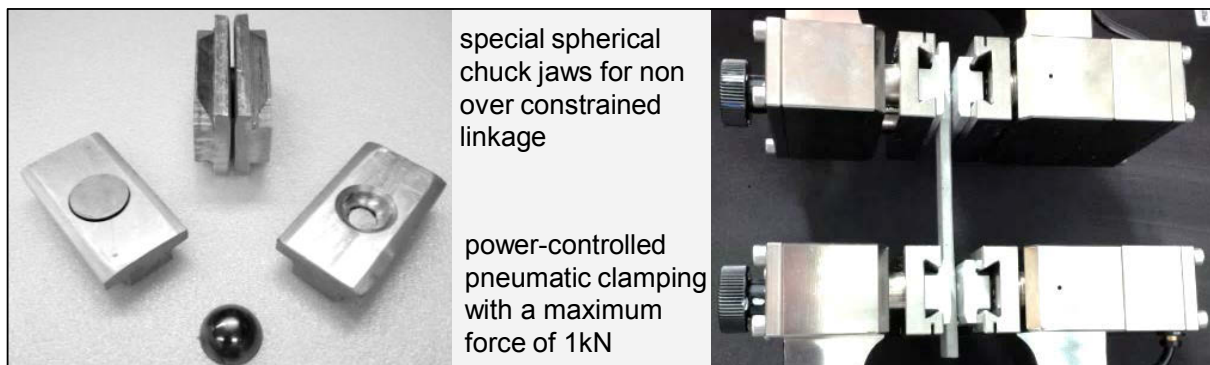

special spherical chuck jaws for non over constrained linkage

power-controlled pneumatic clamping with a maximum force of 1kN

Figure 4. Tensile test arrangement at the ZWICK Roell Z010

Since the clamping is pneumatically controlled, the lateral force applied by the clamping is reproducible even if the cross-sections in a lot are different in height. The clamping force is constant at a level of 1 kN.

4.1.3 3-point bending test arrangement

Concrete parts are characterized by a high sensitivity to lateral loads and shear stresses. To reduce the influences of the arrangement over-constraints in the specimen treatment needs to be avoided. To realize a 2D modeled 3-point bending test with 3D specimen of rectangular cross section, which are containing geometrical errors, linear contact elements are useful. This is possible with three cylindrical pins made of steel. For a well constraint situation two of the pins have to rotate free around the beam axis. Since the rolling axis is coincident to the beam's surface which is in contact to the fixed pin the contact friction is minimized.
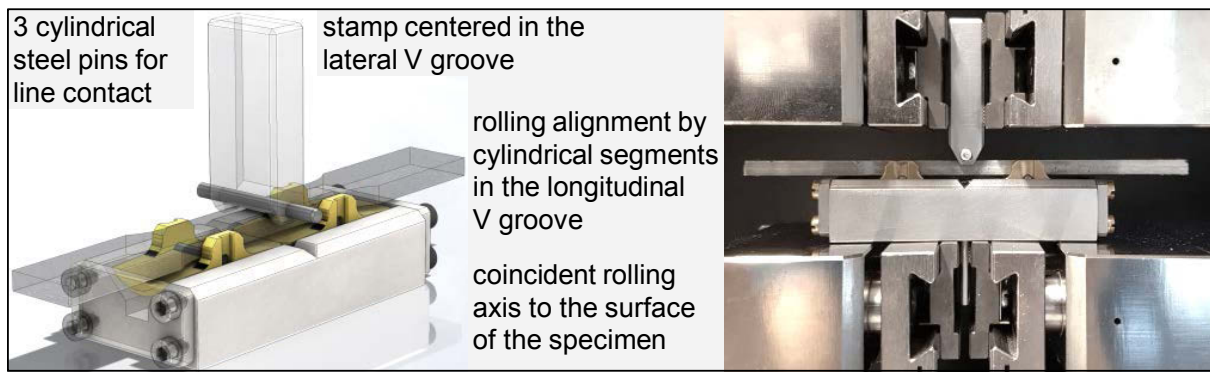
Figure 5. *Bending test arrangement at the ZWICK Roell Z010*

In figure 5 the bending test arrangement is shown. To achieve highly reproducible results the symmetry and the orthogonal alignment is essential. The setup of the testing machine is done within the following three steps:

1. The frame part with the longitudinal V groove is fixed at the bottom clamp
2. The stamp is put into the lateral V groove
3. The adjustable chuck of the top clamp is moved till the contact to the stamp is planar

Now both sides of the bearing carrying cylindrical segments can be put in.

The horizontal position of the specimen is fixed by the cylindrical segments with a tolerance of ±0.5 mm, that the angular tolerance is less than 1.6° for the linear pin contacts. The parallel specimen length is about 45 mm. So the longitudinal position is not critical.

4.1.4 *Indirect measurement of the specimen displacement*

For the investigation of new sol-gel-compositions a high number of specimens are needed. Statistical confident results are possible with a minimum of 6 specimen of each state. Due to tolerances in geometry and non-reproducible porosity 10 specimen of each state are tested for the tensile and the flexural load. To reduce the operative effort for the tests it is obvious to take the displacement measurement by the internal system of the testing machine. The specimen displacement is calculated in consideration of the in-line arrangement of the machine stiffness and the specimen stiffness. The determination of the machine stiffness is done by measurements with specimen of vastly higher high stiffness.

The length of interest to determine the tensile stiffness or the Young's modulus is about 35 mm of the parallel specimen length L. With the information of the machine stiffness the calculation of the clamping displacement with the distance A (figure 3) of the centers is possible. To validate the elongation of L a transmission factor for the implication of the cross-section is needed. In figure 6 an exemplary simulation considering the clamping situation and the qualitative specimen deformation is shown.
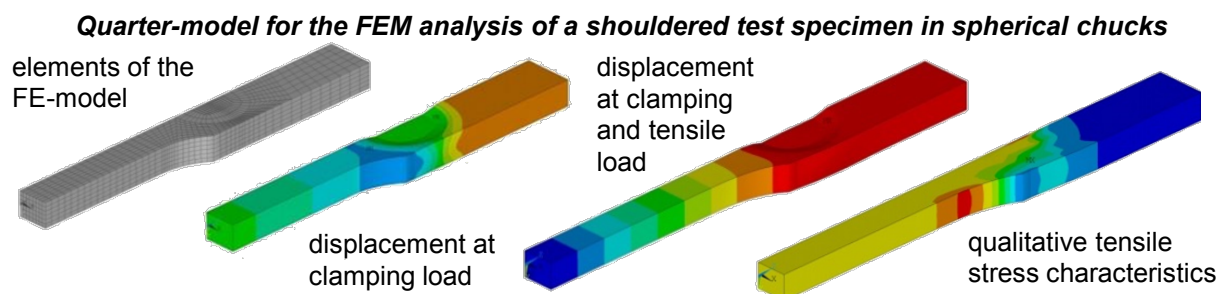

Figure 6. *Qualitative FEM solution results with respect to the clamping force and the tensile load*

The second picture from the left shows the clamping situation without an additional longitudinal load. After the clamping a compression load according to the replacement of the spherical clamps is resulting at the load cell. After tensile load application the longitudinal displacement in L amounts to 54.68% of A for the chosen clamping force of 1 kN. . Therefor the transmission factor between displacements of the clamping and expansion length of L is set to the value 0.5468.

4.1.5 Testing machine ZWICK Roell Z010

The ZWICK Roell Z010 is a material testing machine for desktop installation. To characterize the uncertainty coming up with the machine parameters the guide to the expression of the measurement uncertainty (GUM) is used. In figure 7 the systematical procedure is shown.

Parameters for the stiffness determination

$C_{specimen}$	= stiffness of the specimen	X	= displacement factor
C_{mach}	= stiffness of the test arrangement	F	= applied force load
s_{norm}	= displacement of the specimen	L	= parallel length of the specimen
s_{maes}	= overall displacement	A	= distance between the spherical clamps

Tensile test stiffness determination

$$C_{specimen} = \frac{F}{s_{norm}} = \frac{A}{XL\left(\frac{s_{maes}}{F} - \frac{1}{C_{mach}}\right)}$$

Bending test stiffness determination

$$C_{specimen} = \frac{F}{s_{norm}} = \frac{1}{\left(\frac{s_{maes}}{F} - \frac{1}{C_{mach}}\right)}$$

Tolerances in the measurement system

U_{CS} = specimen stiffness uncertainty
U_{CM} = test arrangement stiffness uncertainty
$\Delta s, \Delta A$ = machine reproducibility = $\pm 2\mu m$

ΔX = Ø (constant factor validated by FEM)
ΔF = 0.05%..0.15% (load cell class I in ISO376)
ΔL = Ø (standard length for evaluation)

test arrangement stiffness uncertainty ($C_{specimen} \rightarrow \infty$)

$$U_{CM} = \sqrt{\left(\frac{\partial C_{mach}}{\partial F}\Delta F\right)^2 + \left(\frac{\partial C_{mach}}{\partial s_{maes}}\Delta s\right)^2} = C_{mach}\sqrt{(\Delta F \cdot F)^2 + \left(\frac{\Delta s}{s_{maes}}\right)^2}$$

specimen stiffness uncertainty

$$U_{CS} = \sqrt{\left(\frac{\partial C_{specimen}}{\partial A}\Delta A\right)^2 + \left(\frac{\partial C_{specimen}}{\partial F}\Delta F \cdot F\right)^2 + \left(\frac{\partial C_{specimen}}{\partial s_{maes}}\Delta s\right)^2 + \left(\frac{\partial C_{specimen}}{\partial C_{mach}}U_{CM}\right)^2}$$

$$U_{CS} = \frac{1}{XL\left(\frac{s_{meas}}{F} - \frac{1}{C_{mach}}\right)}\sqrt{\left[\left(s_{meas-}\frac{F}{C_{mach}}\right)\Delta A\right]^2 + (\Delta F \cdot F)^2 + (A\Delta s)^2 + \left(\frac{AF}{C_{mach}}U_{CM}\right)^2} \quad (*)$$

(∗) for the bending load case the parameters (X, L, A) = 1 and ΔA = Ø

Figure 7. *Systematic measurement uncertainty following GUM*

4.2 Experimental results

4.2.1 Determination of the infiltrated depth and the wall thickness of the coating

The measurements for the coating influenced dimensions actually do not show any convenient results. The main problem is the visibility of the gel into the concrete. Some test cubes dip coated in $SnCl_2$ were tested by X-ray fluorescence. Sn and Cl were found on the surface.

Inside the concrete specimen no components fluorescent solutions could be determined. Actually a measurement of the infiltrated depth is not possible with this setup.

Currently it is also difficult to determine the coating thickness, because the transition from coating to non-coating surface is still too rough. The measured thicknesses fluctuate between 450 and 1000 nm. In the exemplary profile graph shown in figure 8 a thickness of 500 nm was determined.
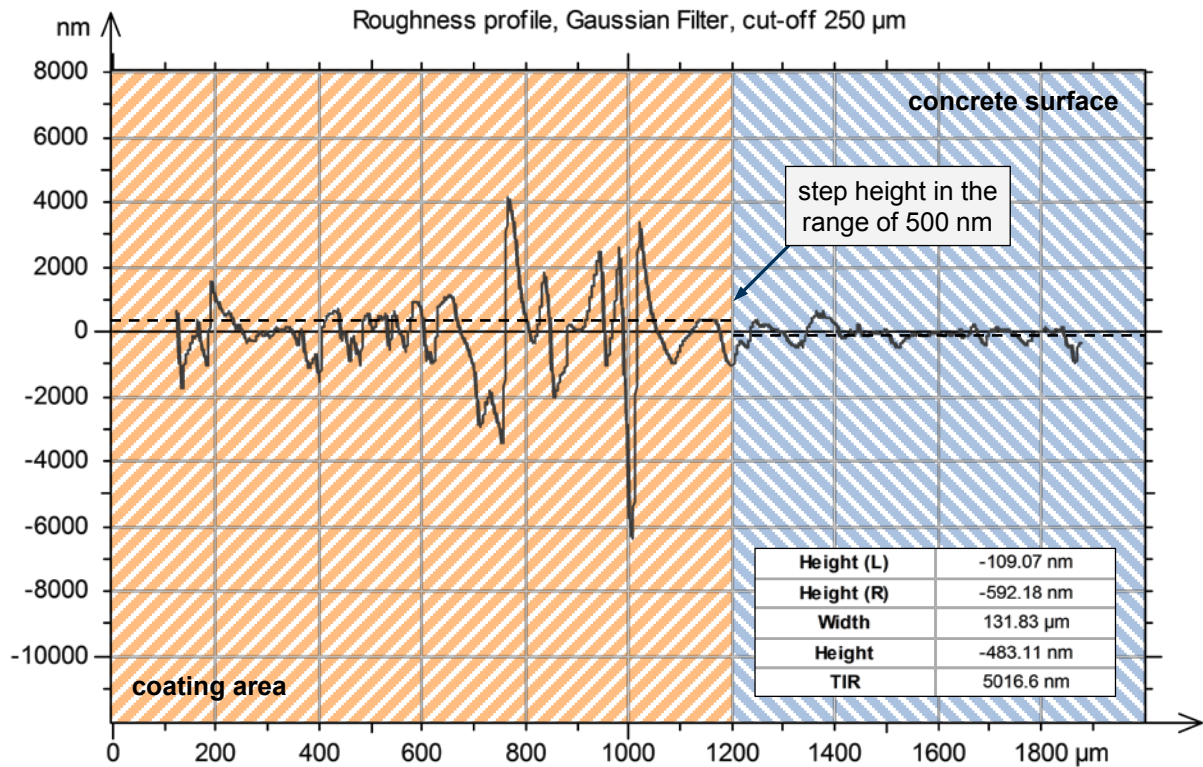

Figure 8. Exemplary thickness measurement profile

4.2.2   Determination of the testing machine stiffness's for tensile and flexural arrangement
The overall machine stiffness is influenced by all the in-line components except of the specimen itself. To investigate the test arrangements stiffness specimen of significant higher stiffness were used. For the tensile machine stiffness a specimen made of steel with a cross section of 6x40 mm² were used. The flexural stiffness was determined with a steel specimen 10 mm in width and 20 mm in height.
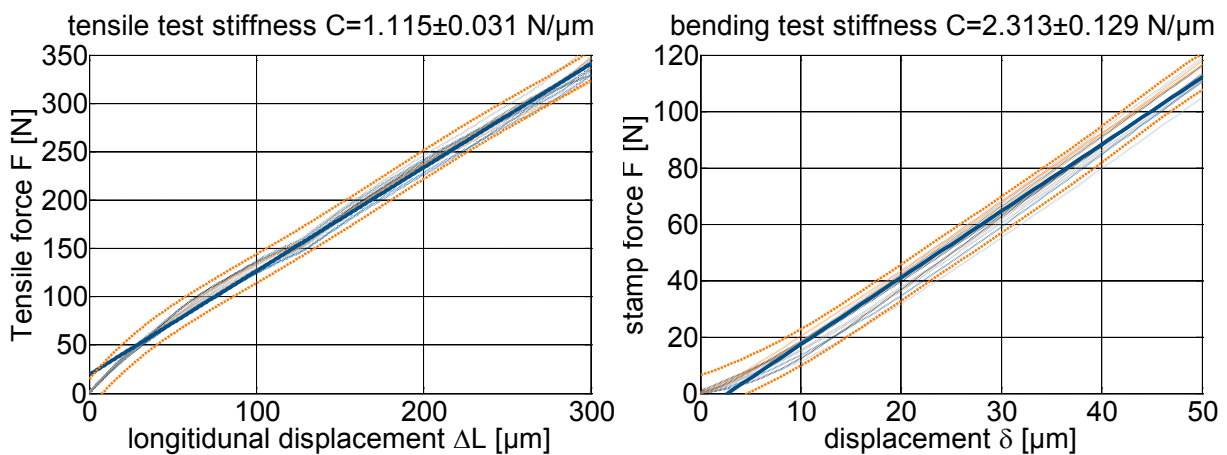

Figure 9. Machines over all stiffness's left for tensile load and right for bending load test

The deviation at the tensile load curve shown in figure 9 is induced by a setting effect in the clamp. This effect is highly reproducible and could be corrected in the analysis procedure. The progressive behavior at lower forces in the bending test diagram could be caused by the Hertz contact at the cylindrical pins.

4.2.3   Determination of the stiffness and the Young's modulus of the uncoated beams

In the stress-strain-diagram at figure 10 the characteristics of some uncoated (label xxxx) beams are shown. This data is used to determine the Young's modulus of the base material.
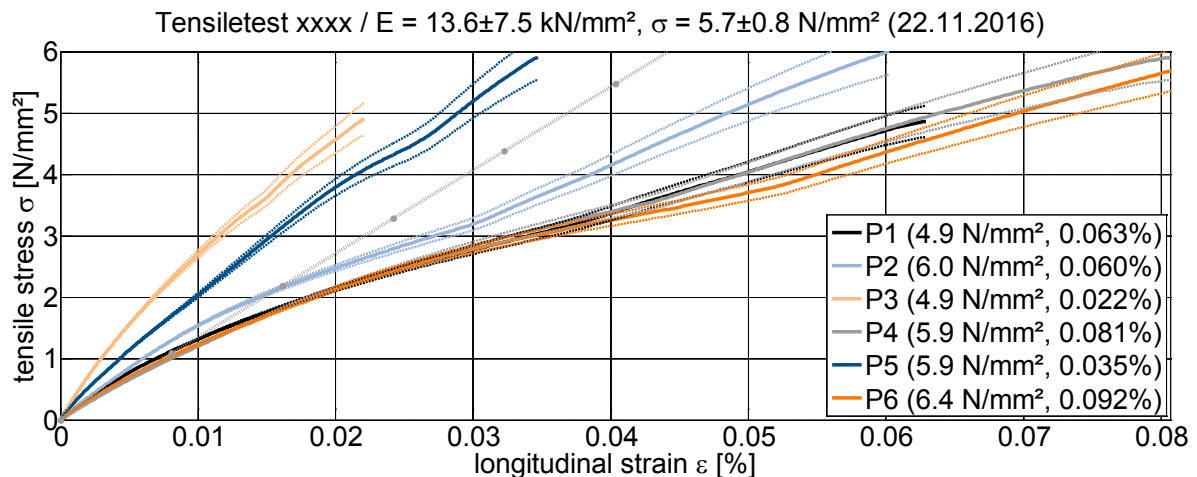

Figure 10. Determination of the Young's modulus of the uncoated beams

The presently high level of variation does not allow a reliable prediction of the efficiency of the sol-gel coating. For that reason and for a better clarity only the systematic error of the test machine arrangement is shown in the following sections. Investigations have been done at medium level to avoid effects at minimum and maximum force loads.

4.2.4   Characterization of the influence of different Sol-Gel coatings

For the tensile load see figure 11 the coatings with V26e and V24b are very promising for the stiffness improvement and the following enhancement of endurance strength. The sol-gel variations V13f and V18b are not useful to achieve an endurance strength enhancement.
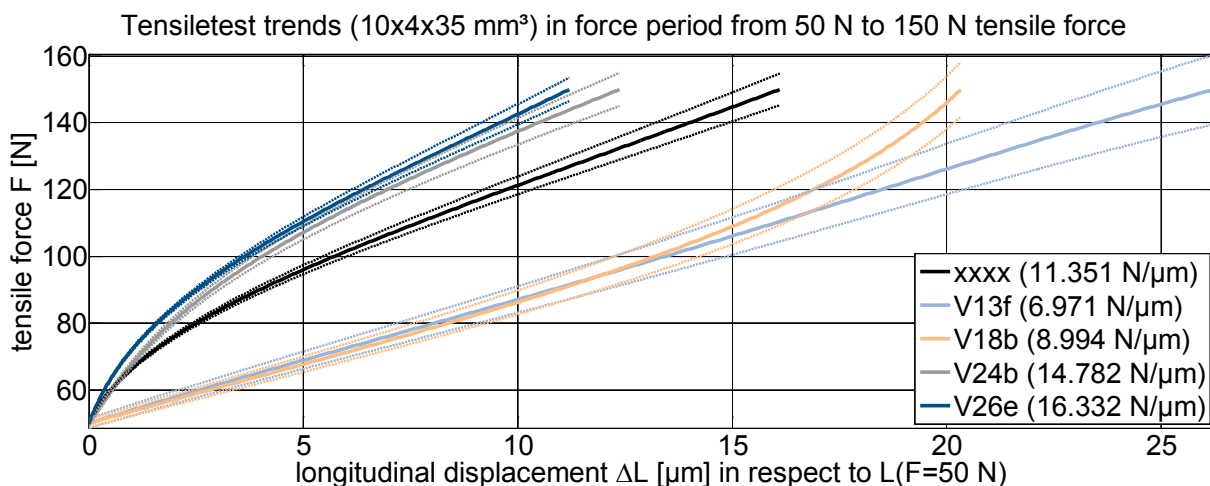

Figure 11. Stiffness trends for the tensile load with systematical error borders for 3σ

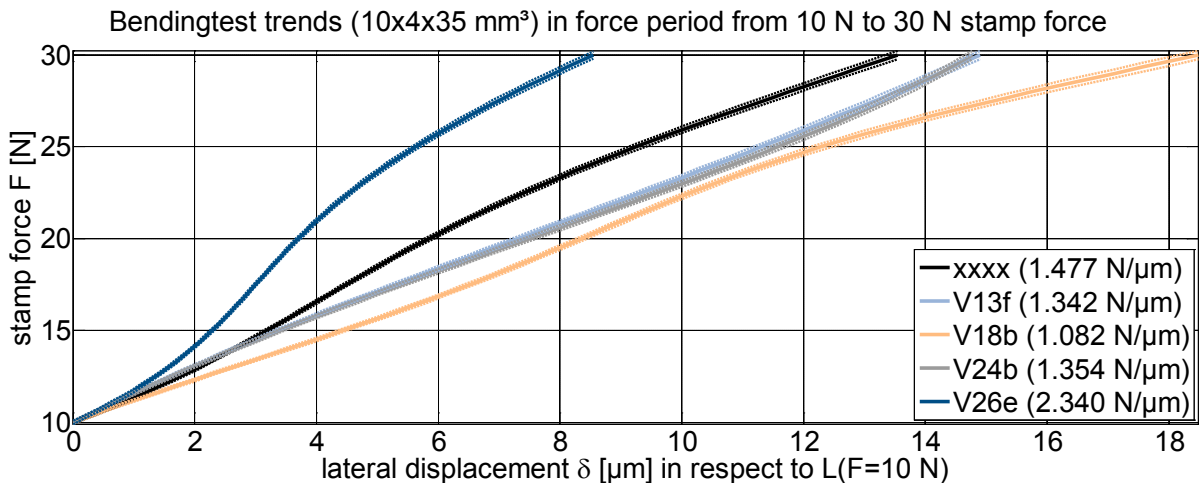The coating V26e (figure 12) yields promising stiffness improvement for the bending load.

Figure 12. *Stiffness trends for the flexural load with systematical error borders for 3σ*

5. PHYSICAL PROPERTIES [1]

If the measured geometrical dimensions (B, H, T, RHT), the Young's modulus E_0, the tensile stiffness $C_{tensile}$ and the flexural stiffness $C_{flexure}$ are known, the determination of the Young's modulus E_1 and E_2 could be done. An infinitely number of combinations of E_1 and E_2 have equal stiffness to each measurement. The equal stiffness lines can be expressed in an E_1-E_2-diagram shown in figure 13 for the exemplary Young's modulus contribution of figure 2 and the shell element properties (T_{subst}, E_{subst}) can be calculated.
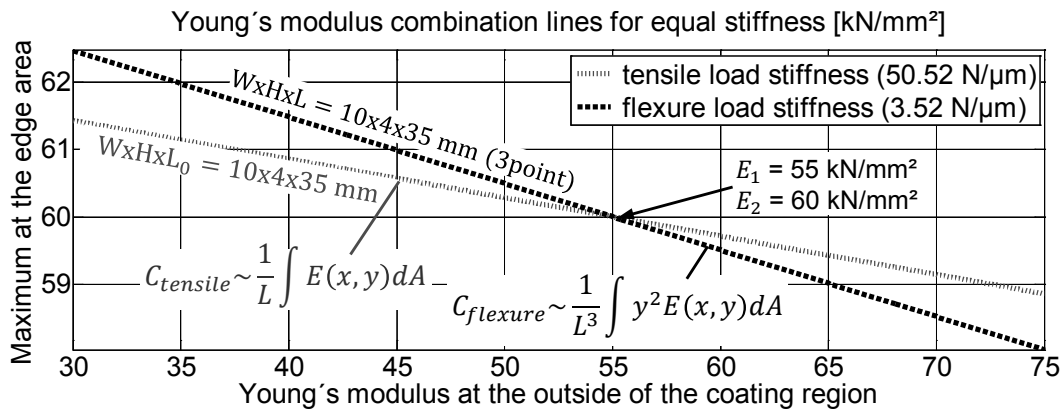

Figure 13. *E_1-E_2-diagram with lines for equal stiffness's for tensile an flexural load*

6. ENDURANCE STRENGTH ENHANCEMENT

With the surface shell elements the stiffness prediction for complex light-weight geometry with sol-gel coating with the representative shell elements could be done in a very easy way. The <u>minimum</u> enhancement of the endurance strength is the offset of the Wöhler curve caused by the reduced relative strain level.

$$X = \frac{N_{coated}}{N_{uncoated}} = \left(\frac{\sigma_{coated}}{\sigma_{uncoated}}\right)^{-k} \quad \blacktriangleright \quad C \sim \frac{1}{\sigma} \quad \blacktriangleright \quad X = \left(\frac{C_{uncoated}}{C_{coated}}\right)^{-k}$$

N = cycles to failure
k = Wöhler coefficient
σ = stress
C = stiffness

Figure 14. *Endurance strength enhancement factor X [7]*

The endurance strength enhancement can be defined by the factor X shown in figure 14. Furthermore the flattening of the Wöhler curve leads to even higher endurance strength. This effect has to be investigated experimentally in dynamic tests. The consideration of this effect could be done with a customized Wöhler coefficient.

7. CONCLUSION

The efficiency of the sol-gel application on concrete parts to achieve stiffness improvement has been proven. A consistent approach for the calculation of the endurance strength enhancement has been shown [1]. An optimization of the manufacturing process of the test specimen is needed to minimize the instability of the results of the mechanical tests. If the distributions of the mechanical parameters of the test specimens are in the magnitude of the uncertainty of the test arrangement, statistical reliable results are possible. The determination of the coating dimensions (infiltration depth and coating thickness) is the main challenge to solve at future investigations.

REFERENCES

[1]   C. Hahm,   R. Theska: D. Raab,   A. Fehringer,   A. Kästner, "Strength enhancement of precision concrete parts by sol-gel surface coating" , euspen's 17th International Conference & Exhibition, Hannover, May 2017

[2]   C. Hahm, R. Theska, "Concrete parts with replicated air bearing path ways", 2nd Gas Bearing Workshop, Düsseldorf, March 2017,

[3]   A. Flohr, A. Dimmig-Osburg, C. Hahm, R. Theska, „Sonderbetone für den Präzisionsmaschinenbau", Concrete Plant International, September 2014

[4]   C. Hahm,   R. Theska,   A. Flohr,   A. Dimmig-Osburg,   O. Hartmann: "Concrete – Future Material for High Precision Machines", 58th Ilmenau Scientific Colloquium, Ilmenau, September 2014

[5]   C. Hahm,   R. Theska,   K. John,   A. Flohr,   A. Dimmig-Osburg, "Concrete Based Parts for High Precision Applications", 13th International Conference & Exhibition, Berlin, May 2013

[6]   M. Berg,   R. Bernau,   T. Erbe,   K. Bode,   R. Theska, "Primary shaping of smooth and level guideway planes for high precision applications", 10th International Conference & Exhibition, Delft, May 2010

[7]   Forschungskuratorium Maschinenbau (FKM) 2012 „FKM Richtlinie - Rechnerischer Festigkeitsnachweis für Maschinenbauteile aus Stahl, Eisenguss- und Aluminiumwerkstoffen", VDMA Verlag GmbH, Frankfurt am Main, 2012

CONTACTS

C. Hahm *christoph.hahm@tu-ilmenau.de*
Prof. Dr.-Ing. R. Theska rene.theska@tu-ilmenau.de